Tumor Biol. (2015) 36:3919–3930
DOI 10.1007/s13277-014-3035-1

RESEARCH ARTICLE

Indole-3-carbinol suppresses NF-κB activity and stimulates the p53 pathway in pre-B acute lymphoblastic leukemia cells

Majid Safa · Behnaz Tavasoli · Rima Manafi · Fatemeh Kiani · Meysam Kashiri · Saber Ebrahimi · Ahmad Kazemi

Received: 6 October 2014 / Accepted: 30 December 2014 / Published online: 15 January 2015

Abstract B cell precursor acute lymphoblastic leukemia (BCP-ALL) is the most common type of cancer in children. Dramatic improvements in primary therapy for childhood ALL have led to an overall cure rate of 80 %, providing opportunities for innovative combined-modality strategies that would increase cure rates while reducing the toxic side effects of current intensive regimens. In this study, we report that indole-3-carbinol (I3C), a natural phytochemical found in cruciferous vegetables, had anti-leukemic properties in BCP-ALL NALM-6 cells. I3C induced cell growth inhibition by G1 cell cycle arrest and triggered apoptosis in a dose- and time-dependent manner. p53, p21, and Bax proteins showed increased expression after I3C treatment. Real-time PCR analysis of pro-apoptotic p53 target genes revealed up-regulation of PUMA, NOXA, and Apaf-1. I3C also suppressed constitutive nuclear factor-κB (NF-κB) activation and inhibited the protein expression of NF-kappa B-regulated antiapoptotic (IAP1, Bcl-xL, Bcl-2, XIAP) and proliferative (c-Myc) gene products. Coadministration of I3C with the topoisomerase II inhibitor, doxorubicin, potentiates cytotoxic effects compared with either agent alone. Apoptosis induction by the drug combination was associated with enhanced caspase-9 activation and PARP cleavage. Furthermore, I3C abolished doxorubicin-induced NF-κB activity as evidenced by decreased nuclear accumulation of p65, inhibition of IκBα phosphorylation and its degradation, and decreased NF-κB DNA-binding activity. Western blot analysis revealed that doxorubicin-induced Bcl-2 protein expression was inhibited by I3C. Overall, our results indicated that using nontoxic agents, such as I3C, in combination with anthracyclines might provide a new insight into the development of novel combination therapies in childhood BCP-ALL.

Keywords Indole-3-carbinol · Acute lymphoblastic leukemia · NF-κB · p53 · Doxorubicin

Introduction

Acute lymphoblastic leukemia (ALL) is the most common childhood malignancy accounting for almost 30 % of pediatric cancers. It has a peak incidence at 2 to 5 years of age, but also occurs, albeit with low incidence, in adults and the elderly [1]. Despite high cure rates for ALL, resistance to treatment and disease relapse remain a significant problem. Understanding the mechanisms by which chemoresistance can occur is therefore important for developing novel therapeutic approaches aiming to improve patient survival [2, 3]. Leukemic cells exhibit uncontrolled proliferation mostly due to aberrantly regulated cell survival and apoptosis signaling pathways [4]. TP53 is the most common tumor suppressor gene mutated in all human cancers which is associated with poor prognosis and drug resistance [5]. Interestingly, in pediatric ALL, the incidence of TP53 mutation is considerably low [6], reflecting the fact that wild-type p53 harboring ALL cells can be

M. Safa (✉) · A. Kazemi
Cellular and Molecular Research Center, Iran University of Medical Sciences, Tehran, Iran
e-mail: safa.m@iums.ac.ir

A. Kazemi
e-mail: a.kazemi@iums.ac.ir

M. Safa · B. Tavasoli · A. Kazemi
Department of Hematology, Faculty of Allied Medicine, Iran University of Medical Sciences, Tehran, Iran

R. Manafi · F. Kiani · M. Kashiri · S. Ebrahimi
Department of Hematology, School of Allied Medical Sciences, Tehran University of Medical Sciences, Tehran, Iran

targeted by agents that activate p53 signaling pathway [7]. In contrast to activation of p53, which is associated with the induction of apoptosis, stimulation of nuclear factor-κB (NF-κB) has been shown to promote resistance to apoptosis [8, 9]. NF-κB consists of p50 and p65 heterodimer retained in the cytoplasm by inhibitory proteins called IκBs. In response to many stimuli, IκB kinase (IKK) is activated, leading to IκBα phosphorylation, ubiquitination, and degradation by the proteasome. The liberated p50-p65 complex then translocates to the nucleus, binds to its consensus sequence within the promoter of NF-kB target genes, and regulates gene transcription [10, 11]. A group of antiapoptotic genes, including Bcl-xL, cIAP1, cIAP2, XIAP, Bcl-2, c-FLIP, and TRAF-2, can be up-regulated by NF-κB, underlining its importance on cell death in cancer cells [12, 13]. Persistent and prolonged activation of NF-κB has been observed in several types of cancer where it is believed to induce gene products that allow these cells to evade apoptosis [14, 15]. Constitutive NF-κB activation occurs in over 90 % of childhood ALL tumors and strongly suggests a critical role of this factor for leukemia cell survival either by blocking apoptosis or by enhancing proliferation [16]. Thus, there are compelling reasons to believe that subverting NF-κB function would be an effective strategy to restore or enhance apoptosis in ALL cells. Much evidence indicates that various natural compounds exhibit an anticancer effect through perturbing multiple cellular signaling pathways [17]. Indole-3-carbinol (I3C), a natural compound present in cruciferous vegetables such as broccoli and cabbage, is a promising anticancer phytochemical [18]. In various cancer cells, I3C has exhibited anticancer effects, including cell cycle inhibition, apoptosis, and decreasing tumor invasion through modulation of cellular signals such as NF-κB, p53, Akt, and JNK pathways [19–21]. However, the effect of I3C on B cell precursor acute lymphoblastic leukemia (BCP-ALL) cells, the most predominant subtype in all age groups of ALL, has not yet described. In the present study, we investigated the effects and the molecular mechanism of I3C on growth and apoptosis in BCP-ALL-derived cell line NALM-6. We show that treatment of NALM-6 cells with I3C induces apoptosis in a dose- and time-dependent manner. In addition, I3C down-regulates the expression of antiapoptotic NF-κB target genes and activates p53 signaling pathway. Cotreatment of I3C with doxorubicin dramatically increased apoptosis in NALM-6 cells.

Material and methods

Cell culture

NALM-6 cells (human B cell precursor acute lymphoblastic leukemia cell line) were grown in suspension in RPMI medium supplemented with 2 mM L-glutamine, 10 % FBS, 100 units/ml penicillin, and 100 μg/ml streptomycin in a humidified 5 % CO_2 incubator at 37 °C under standard cell culture conditions.

Cell proliferation assay

The effect of various concentrations of I3C on metabolic activity of NALM-6 cells was assessed by the MTT colorimetric method. MTT is reduced to an insoluble formazan dye by mitochondrial enzymes associated with metabolic activity. Actively proliferating cells increase their metabolic activity while cells exposed to cytotoxic drugs will have decreased activity. Briefly, exponentially growing cancer cells were seeded into a 96-well culture plate at a density of 10×10^3 cells/well and incubated with various concentrations of I3C for 24 and 48 h. After removing the medium, cells were incubated with MTT solution (5 mg/ml in PBS) for 4 h and the resulting formazan was solubilized with DMSO (100 μl). The absorbance of each well was measured at 570 nm in an ELISA reader.

Sub-G1 DNA content analysis

Apoptotic cells were detected using PI staining of I3C-treated cells followed by flow cytometry to detect the so-called sub-G1 peak. Briefly, NALM-6 cells were seeded into six-well plates at the concentration of 1×10^6 cells/well and incubated with different concentrations of I3C for indicated hours. NALM-6 cells were then harvested and washed twice with PBS and fixed with 70 % ethanol. Then cells were treated with 0.5 μg/ml RNase in PBS and incubated at 37 °C for 30 min before staining with 50 μg/ml PI for 30 min. The cells were analyzed using a FACScan flow cytometer (Becton Dickinson).

Phosphatidylserine externalization (annexin-V assay)

NALM-6 cells were treated with doxorubicin in the presence or absence of different concentrations of I3C for 24 h and were then washed with PBS after the incubation time. A total of 1×10^6 cells per sample were resuspended in a total volume of 100 μl of the incubation buffer. Annexin-V-Flous (2 μl per sample) was added, and cell suspensions were incubated for 20 min in the dark. Fluorescence was then measured using flow cytometery. The data were evaluated using the CellQuest Software (Becton Dickinson) and expressed as percentage of the cells positive for annexin-V (early apoptotic phase).

RNA purification, reverse transcription, and real-time PCR amplification

Total RNA was isolated from the cells using TriPure isolation reagent (Roche), according to the manufacturer's instructions. One microgram RNA was used to prepare cDNA using the

RevertAid First Strand cDNA Synthesis kit from Fermentas. The cDNA prepared was subjected to quantitative reverse-transcriptase polymerase chain reaction (qRT-PCR), using Maxima SYBR green master mix (Fermentas) in the Rotor Gene 6000 Real Time PCR System (Corbett Research, Hilden, Germany). DNA was amplified in a 40-cycle PCR reaction with the following conditions: denaturation at 95 °C for 15 s, annealing and elongation at 60 °C for 60 s. The fold induction or repression was measured relative to control and calculated after adjusting for reference gene GAPDH. Each sample was analyzed in triplicate, and representative data sets are shown. Primer sequences are given as follows: PUMA (forward: gacctcaacgcacagtacgag, reverse: aggagtcccatgatgagattgt), NOXA (forward: ccgtgtgtagttggcatctc, reverse: cccactcagcgacagagc), APAF-1 (forward: acaatgctctactacatgaaggatataaaga, reverse: cactggaagaagagacaacaggaa), hTERT (forward: atgcgacagttcgtggctca, reverse: atcccctggcactggacgta), GAPDH (forward: gaaggtgaaggtcggagtc, reverse: gaagatggtgatgggatttc).

Western blot analysis

Cells were centrifuged at different time points after various treatments, and cellular pellets were washed with cold PBS and lysed (5×10^6 cells/aliquots) in 0.2 ml of RIPA buffer (10 mM Tris-HCl, pH 7.4, 150 mM NaCl, 5 mM EDTA, 1 % Triton X-100, 0.1 % sodium dodecyl sulfate, and 0.5 % sodium deoxycholate) containing protease and phosphatase inhibitor cocktails (Sigma). After centrifugation at 13,000×*g* for 20 min at 4 °C, the supernatant was collected. Protein concentrations were determined by Bradford protein assay, and equivalent amounts of total cellular protein were separated by 10 % SDS-PAGE, according to the method of Laemmli. The gels were then electroblotted onto nitrocellulose membranes (Hybond-ECL, Amersham Corp.). Subsequently, membranes were blocked with 5 % nonfat dry milk in TBS containing 0.1 % (*v*/*v*) Tween-20 for 1 h at room temperature and probed with specific primary antibodies overnight at 4 °C. After five washes in TBS-T, membranes were incubated with HRP-conjugated secondary antibodies. Proteins were then visualized with a chemiluminescence detection system (Amersham ECL Advance Kit, GE Healthcare). Densitometric quantification was done using ImageJ software.

Nuclear fractionation and NF-κB p65 DNA-binding activity assay

The preparation of nuclear extracts was performed using the Nuclear Extract Kit (Active Motif, Carlsbad, CA) according to manufacturer's instructions. The DNA-binding activity of NF-κB was quantified in the NALM-6 cells by TransAMTM NF-κB p65 Transcription Factor Assay Kit (Active Motif, TransAM® NFκB p65, #40096) according to the manufacturer's instructions. Briefly, 5 μg of the nuclear extracts was incubated in 96-well plates coated with immobilized oligonucleotide (5′-AGTTGAGGGGACTTTC CCAGGC-3′) containing a consensus (5′-GGGACTTTCC-3′) binding site for the p65 subunit of NF-κB for 1 h. NF-κB binding to the target oligonucleotide was detected by incubation with primary antibody specific for p65 subunit. HRP-conjugated secondary antibodies were used for the detection of p65 bound to the target oligonucleotides. For quantification of NF-κB activity, the optical densities were measured at 450 nm by a microplate reader.

Statistical analysis

Data were analyzed using a two-tailed Student's *t* test. A *P* value of <0.05 was considered statistically significant.

Results

I3C induces cell-growth inhibition, G1 cell-cycle arrest, and apoptosis in NALM-6 cells

To test the effects of I3C on cell growth, we treated NALM-6 cells with 20, 30, 40, 50, and 60 μM I3C for 24 and 48 h. It is well known that actively proliferating cells increase their metabolic activity. In Fig. 1a, we show I3C's dose-dependent inhibition of metabolic activity of NALM-6 cells. Inhibition of cell proliferation could be the result of the induction of apoptosis or cell cycle growth arrest. To determine whether the inhibitory effects of I3C on cell proliferation could be attributed to alterations in the cell cycle, NALM-6 cells were treated with different concentrations of I3C for 24 h and subjected to cell cycle analysis by flow cytometry. We found that in NALM-6 cells, increasing concentrations of I3C induced the percentage of G1 phase cells (Fig. 1b). Moreover, to ascertain whether the cell death induced by I3C could be apoptosis, we investigated the cleavage of poly (ADP-ribose) polymerase (PARP) or activation of caspase-3, caspase-7, and caspase-9 by western blotting after treatment of NALM-6 cells with different concentrations of I3C for 24 and 48 h. As shown in Fig. 1c, I3C alone activated these caspases and cleaved PARP at maximal concentration (60 μM) obviously after 48 h, and to a lesser extent after 24 h. Caspase activation and PARP cleavage were also observed with lower concentration of I3C (40 μM) treatment for 48 h. Collectively, these results provide evidence that the cell death induced by I3C is caused by cell cycle arrest and caspase-mediated apoptosis.

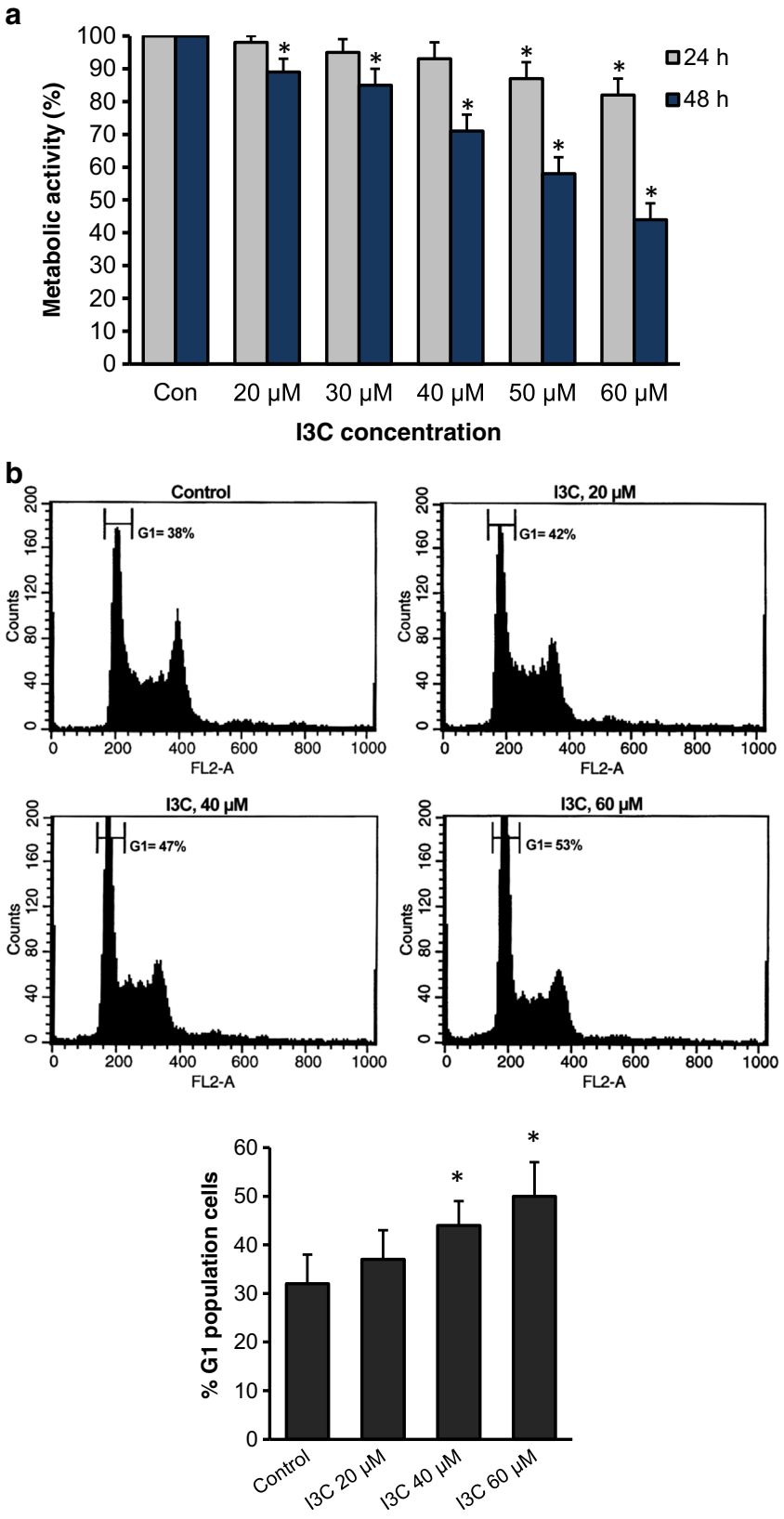
a
Metabolic activity (%)
100
90
80
70
60
50
40
30
20
10
0
24 h
48 h
Con
20 μM
30 μM
40 μM
50 μM
60 μM
I3C concentration
b
Control
G1= 38%
I3C, 20 μM
G1= 42%
I3C, 40 μM
G1= 47%
I3C, 60 μM
G1= 53%
Counts
FL2-A
0
40
80
120
160
200
400
600
800
1000
% G1 population cells
60
50
40
30
20
10
0
Control
I3C 20 μM
I3C 40 μM
I3C 60 μM

◀ **Fig. 1** Effects of I3C on cell proliferation and apoptosis in NALM-6 cells. **a** Cell proliferation assay of NALM-6 cells. Cells were grown in complete medium with different concentrations of I3C in 96-well plates for up to 24 and 48 h, and cell growth was measured by MTT assay. The results are expressed as mean±SD of at least three independent experiments.*$P<0.05$ compared to non-treated control cells. **b** I3C caused cell cycle arrest at G_1 phase. Cells were treated with I3C (20, 40, and 60 μM) for 24 h, and cell cycle analysis was performed by flow cytometry. Data shown are representative of at least three independent experiments.*$P<0.05$ compared to non-treated control cells. **c** Effect of I3C on caspase activation and PARP cleavage. After the treatment of cells with the indicated concentration of I3C for 24 and 48 h, total cell lysates were prepared and western blotting was performed using antibodies specific to cleaved PARP-1, procaspase-3, caspase-9, caspase-7, and β-actin. The *asterisk* represents a nonspecific band seen using the caspase-9 antibody. The relative expression of cleaved PARP protein was calculated by dividing the intensity of each band, quantified using ImageJ, by the respective intensity of actin

I3C induces p53 accumulation and expression of pro-apoptotic p53 target genes

To further understand the molecular mechanism of I3C-induced apoptosis, western blot analysis was performed to study the effect of I3C treatment on the p53 tumor suppressor protein. To do so, NALM-6 cells harboring wild-type p53 were treated with a range of I3C concentrations (0–60 μM) and cells were harvested after 24 and 48 h. p53 protein levels were assessed using western blot analysis of cellular extracts. As presented in Fig. 2a, I3C induced p53 protein levels after 24 and 48 h of treatment with 60 μM I3C producing the highest fold induction of the concentrations tested. Protein levels of the p53 downstream targets p21/waf1 and Bax were also examined by western blot analysis. Treatment of cells with 60 μM I3C resulted in only a modest increase in p21/waf1 and Bax protein levels over control cells after 24 h (Fig. 2a). However, the increase in p21/waf1 and Bax protein levels was prominent after 48 h treatment with I3C 40 and 60 μM. To corroborate these results, we carried out qRT-PCR assays and found that I3C increases mRNA levels of p53-targeted proapoptotic genes including PUMA, NOXA, and Apaf-1 (Fig. 2b). It is known that p53 is a powerful inhibitor of human telomerase reverse transcriptase (hTERT), a key component for telomerase [22]. Indeed, using qRT-PCR, it was shown that I3C repressed hTERT mRNA expression levels in wild-type p53 expressing NALM-6 cells (Fig. 2b).

I3C represses antiapoptotic NF-κB target genes

The constitutive levels of several antiapoptotic NF-κB target genes and the time course for the effect of I3C on expression of these genes in NALM-6 cells were studied by western blot

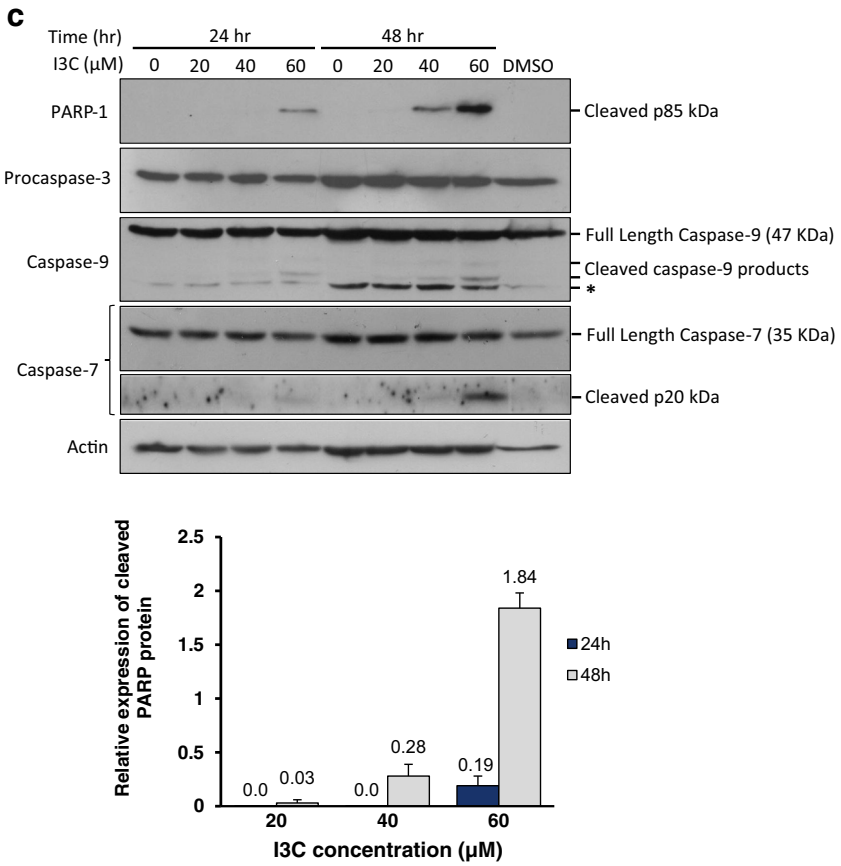

Fig. 1 (continued)

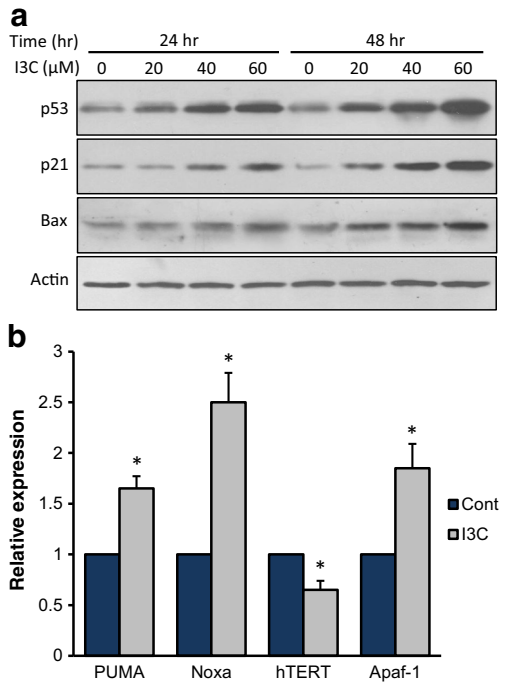

Fig. 2 I3C activates p53-mediated apoptosis pathway. **a** The effect of I3C on the protein expression of p53, p21, and Bax. After the treatment of cells with the indicated concentration of I3C for 24 and 48 h, total cell lysates were prepared and western blotting was performed using antibodies specific to p53, p21, Bax, and β-actin. **b** Modulation of p53 target genes by I3C. NALM-6 cells were treated with 60 μM I3C for 48 h, after which RNA was harvested, and expression of the indicated genes was measured using quantitative RT-PCR and normalized to the expression of GAPDH

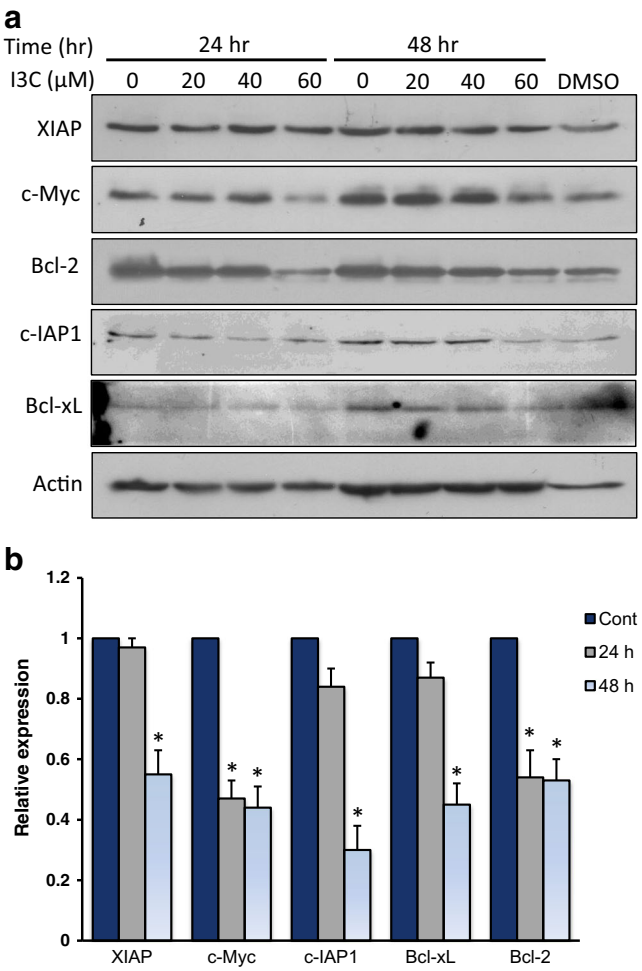

Fig. 3 Effect of I3C on the expression of NF-κB target genes. **a** NALM-6 cells were treated with 20, 40, and 60 μM I3C for 24 and 48 h. Cell lysates were prepared and western blot analysis was performed with indicated antibodies (data from a representative experiment is shown from a total of three independent experiments). **b** Densitometric quantification was done with 60 μM concentration of I3C for 24 and 48 h. The relative expression of the proteins was calculated by dividing the intensity of each band, quantified using ImageJ, by the respective intensity of actin ($n=3$; $^*P<0.05$, relative to untreated cells)

analysis. Cultures of NALM-6 cells were treated with a range of I3C concentrations (0–60 μM) and the protein levels of XIAP, c-Myc, cIAP-1, Bcl-xL, and Bcl-2 were assessed after 24 and 48 h. The levels of c-Myc, Bcl-xL, and Bcl-2 expression were down-regulated in NALM-6 cells treated with 60 μM concentration of I3C for 24 and 48 h (Fig. 3). The protein expression levels of XIAP and c-IAP1 were reduced after treatment of cells with 60 μM concentration of I3C for 48 h.

I3C potentiates doxorubicin-induced apoptosis through caspase activation and PARP cleavage

To determine whether I3C could sensitize BCP-ALL cells to chemotherapeutic drug doxorubicin, we examined the effect of individual and combination treatment with I3C and doxorubicin after 24 h exposure using the MTT assay. We pretreated NALM-6 cells with escalating doses of I3C for 1 h and then with or without 125 nM dose of doxorubicin for further 24 h. As indicated in Fig. 4a, combination of I3C and doxorubicin caused greater inhibition of cellular proliferation than either drug alone. Next, induction of apoptosis was assessed by the annexin-V-staining assay after treatment of cells with doxorubicin and increasing concentrations of I3C for 24 h. We found that I3C could sensitize NALM-6 cells to

Fig. 4 Effects of co-treatment with I3C and doxorubicin on apoptosis in NALM-6 cells. **a** NALM-6 cells were treated with increasing doses of I3C with or without 125 nM doxorubicin (Dox) for 24 h, and the viability of cells was assessed by the MTT assay ($n=3$; $^*P<0.05$, relative to cells treated with either Dox or I3C alone). **b** NALM-6 cells were treated for 24 h with 20, 40, and 60 μM I3C alone, 125 nM doxorubicin alone, or the combinations. Apoptotic cells were quantified using annexin-V-FITC staining and FACS analysis ($n=3$; $^*P<0.05$, relative to cells treated with either Dox or I3C alone). **c** The sub-G1 population was assessed by flow cytometry after exposure to the indicated agents for 24 h. **d** NALM-6 cells were exposed to the indicated agents for 8 or 24 h. The cleavage of PARP and caspase-9 was analyzed by western blotting. β-Actin was used as a loading control. The *asterisk* represents a nonspecific band seen using the caspase-9 antibody

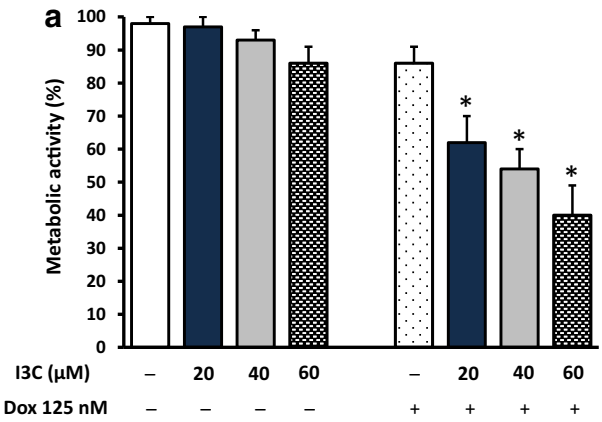
a
Metabolic activity (%)
I3C (μM) – 20 40 60 – 20 40 60
Dox 125 nM – – – – + + + +

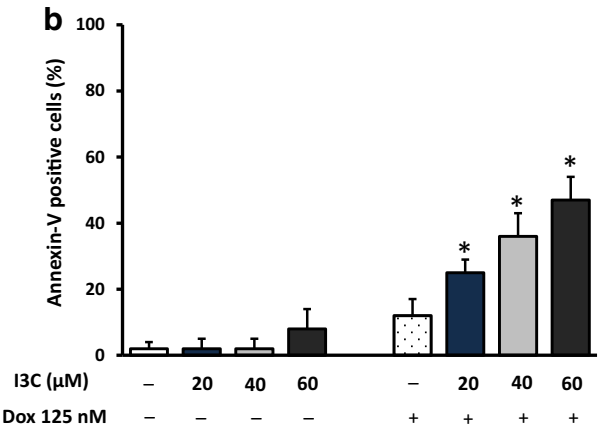
b
Annexin-V positive cells (%)
I3C (μM) – 20 40 60 – 20 40 60
Dox 125 nM – – – – + + + +

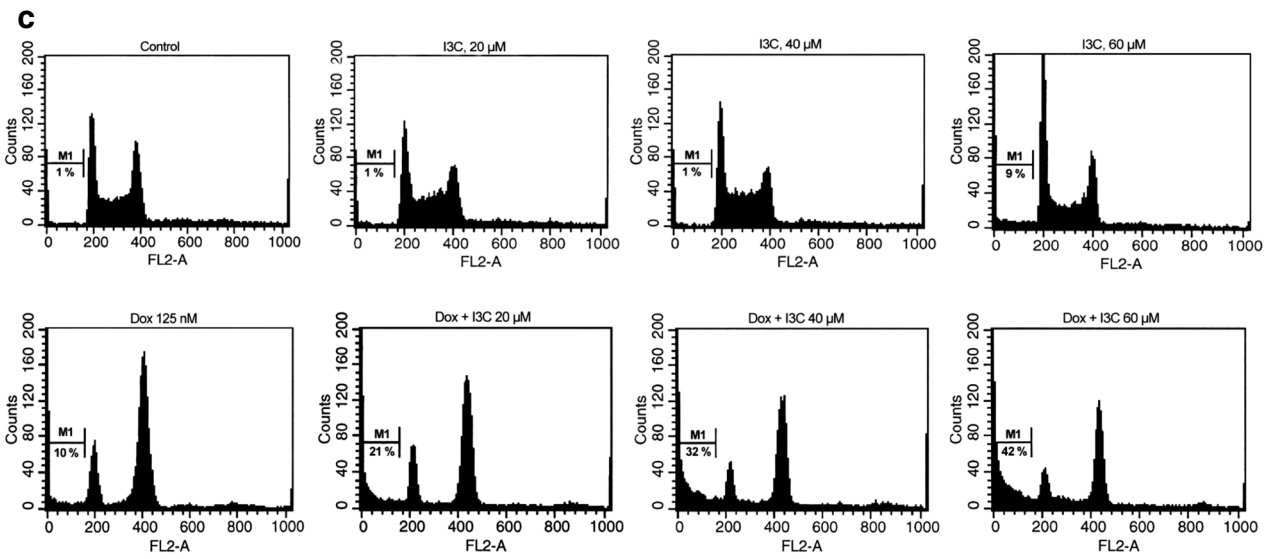
c
Control
I3C, 20 μM
I3C, 40 μM
I3C, 60 μM
Dox 125 nM
Dox + I3C 20 μM
Dox + I3C 40 μM
Dox + I3C 60 μM
Counts
FL2-A
M1
1 %
1 %
1 %
9 %
10 %
21 %
32 %
42 %

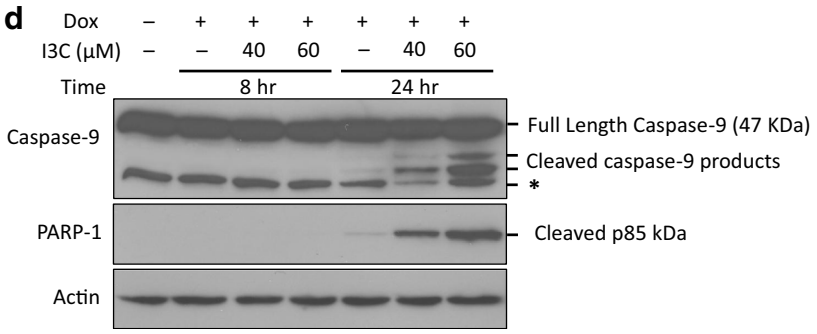
d
Dox – + + + + + +
I3C (μM) – – 40 60 – 40 60
Time 8 hr 24 hr
Caspase-9
PARP-1
Actin
Full Length Caspase-9 (47 KDa)
Cleaved caspase-9 products
*
Cleaved p85 kDa

doxorubicin in a dose-dependent manner (Fig. 4b). Identical drug concentrations used for the annexin-V apoptosis assay were used for cell cycle analysis by flow cytometry. Treatment with increasing concentrations of I3C alone increased the percentage of cells in G1 phase of cell cycle, whereas doxorubicin induced a G2-M arrest in NALM-6 cells (Fig. 4c). In addition, NALM-6 cells treated with combination I3C and doxorubicin exhibited a significant increase in the sub-G1 population indicative of apoptosis (Fig. 4c), consistent with the elevated levels of apoptosis observed in annexin-V assay. To confirm these results at the molecular level, we investigated the cleavage of PARP or activation of caspase-9 by western blotting. It was already shown that I3C by itself had no cytotoxic effect on NALM-6 cells at 40 μM concentration and a minimal cytotoxicity (~10 %) at 60 μM after 24 h. As presented in Fig. 4d, doxorubicin alone could induce only modest PARP and caspase-9 cleavage, whereas in combination with I3C, it clearly cleaved PARP and caspase-9 to their active forms. These data indicate that I3C significantly enhances the apoptotic effect of chemotherapeutic drug doxorubicin in BCP-ALL cells.

I3C inhibits doxorubicin-induced NF-κB activation in NALM-6 cells

A side effect of many commonly used chemotherapeutic drugs is the activation of NF-κB, a potent inducer of antiapoptotic genes, which may mediate the process of chemoresistance in tumor cells [23]. In this study, we have assessed the effect of doxorubicin, an anthracycline widely used in the treatment of hematological cancers including acute lymphoblastic leukemia, in the presence or absence of I3C on NF-κB activation and expression of its downstream target genes Bcl-2 and c-Myc in NALM-6 cells. To this end, cells were pretreated with or without I3C 60 μM for 1 h followed by treatment with doxorubicin 0.25 μM for 4 h, and then the nuclear NF-κB p65 subunit expression and DNA binding were analyzed utilizing western blot analysis and enzyme-linked immunosorbent assay, respectively. As indicated in Fig. 5a, treatment of NALM-6 cells with doxorubicin 0.25 μM resulted in an increase of basal NF-κB p65 DNA binding activity in the nucleus that was markedly reduced in the presence of I3C 60 μM. In order to confirm the results of the p65 DNA binding activity, we also examined the effects of doxorubicin treatment in the presence or absence of I3C on the levels of nuclear p65 by western blot. Consistent with the ELISA results of DNA binding activity, NALM-6 cells treated with doxorubicin for 4 h had a significant increase in nuclear p65 protein when compared to control cells (Fig. 5b). When cells were pretreated with I3C, the ability of doxorubicin to induce nuclear accumulation of NF-κB was inhibited (Fig. 5b). The translocation of NF-κB to the nucleus is preceded by phosphorylation of IκBα and its proteolytic

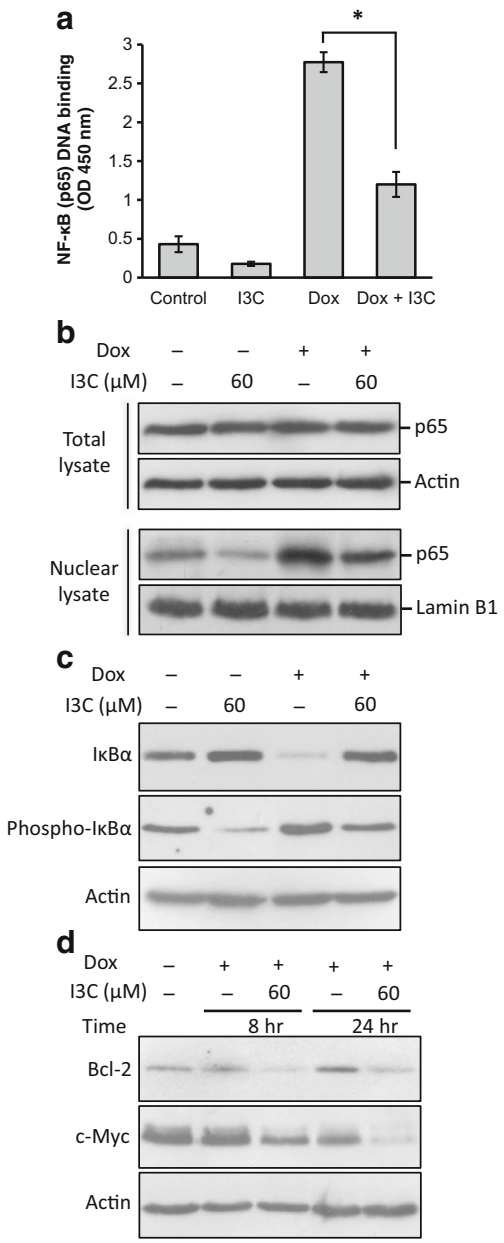

Fig. 5 I3C decreases the induction of NF-κB activity by doxorubicin. **a** NALM-6 cells were treated with or without I3C 60 μM for 1 h before treatment with doxorubicin. The cells were then harvested after 4 h and nuclear fraction was separated using nuclear extraction kit. NF-κB activity was quantified by enzyme-linked immunosorbent assay using the TransAM NF-κB p65 Transcription Factor Assay Kit, according to the manufacturer's instructions. Values represent mean±SD from three independent experiments. **b** NALM-6 cells were pretreated with I3C 60 μM for 1 h prior to adding doxorubicin. Four hours post treatment, the nuclear extracts were collected to detect NF-κB p65 expression by western blotting. **c** NALM-6 cells were pretreated with I3C 60 μM for 1 h prior to adding doxorubicin. After 4 h, the cytoplasmic extracts were collected to detect IκBα and phospho-IκBα proteins by Western blotting. **d** NALM-6 cells were treated with I3C 60 μM before addition of doxorubicin and then harvested at the times indicate. Immunoblot analysis was performed using specific antibodies against c-Myc and Bcl-2. The figure shows one representative blot of three experiments

degradation [24]. To determine whether I3C's inhibitory activity was due to inhibition of IκBα degradation, we pretreated cells with I3C, exposed them to doxorubicin, and examined them for IκBα and phospho-IκBα status by western blot analysis. The I3C-only treated cells showed a dramatic decrease in phospho-IκBα (Fig. 5c). We found that doxorubicin induced IκBα phosphorylation and its degradation, but in I3C-pretreated cells, doxorubicin had no effect on IκBα degradation (Fig. 2b). These results indicate that I3C inhibits both doxorubicin-induced NF-κB activation and IκBα degradation. In addition, the effect of doxorubicin in the presence or absence of I3C on the expression of two known NF-κB target genes, Bcl-2 and c-Myc, was assessed. To this end, cells were pretreated with or without I3C 60 μM for 1 h followed by treatment with doxorubicin 0.25 μM for 8 and 24 h. Cells were then harvested and cellular extracts were evaluated by western blot for the protein levels of Bcl-2 and c-Myc. Exposure to 0.25 μM doxorubicin decreased c-Myc protein expression below constitutive level after 24 h (Fig. 5d). However, c-Myc protein level was further reduced in the presence of I3C. Moreover, the levels of Bcl-2 protein were markedly increased in response to doxorubicin after 24 h that was potently inhibited in the presence of I3C (Fig. 5d). Our results show, when doxorubicin and I3C were combined, c-Myc and Bcl-2 protein levels were substantially decreased, suggesting that I3C can modulate NF-κB target genes through inhibition of NF-κB activity.

Discussion

Emerging evidence suggests that plant-derived dietary compounds and supplements are potential sources of chemicals with anticancer properties that might be combined with chemotherapy or radiotherapy for the more effective treatment of cancer [25–27]. I3C, a naturally occurring component of *Brassica* vegetables such as cabbage, broccoli, and Brussels sprouts, has been shown to reduce the incidence of spontaneous and carcinogen-induced tumors in vivo, and to inhibit the growth of different types of human cancer cells in vitro [28–30]. Recent studies suggest that I3C and its derivatives that prevent cancer may enhance the efficacy of cancer therapeutics through altering the activity of key cell proliferation and survival pathways [18]. Additionally, numerous cell culture, animal, and human studies have demonstrated I3C's safety and tolerability [31, 32]. There is a lot of evidence showing that I3C may find potential application as an adjunctive agent in cancer chemotherapy. Takada et al. showed that I3C (50 μM) potentiates TNF-induced apoptosis through suppression of NF-κB in human acute T cell leukemia Jurkat cell line [33]. In another study, it was shown that I3C (100 μM) enhanced gemcitabine-induced cytotoxicity in pancreatic cancer cells [34]. Furthermore, I3C (100 μM) and tamoxifen have been shown to act cooperatively to inhibit the growth of ER+ breast cancer cells [35]. Nakamura et al. found that combination of I3C (300 μM) and genistein synergistically induces apoptosis in human colon cancer HT-29 cells [36]. In our study, we used 60 μM concentration of I3C to suppress NF-κB and potentiate doxorubicin-induced apoptosis in NALM-6 cells.

We observed that I3C inhibited the growth of BCP-ALL-derived cell line NALM-6 in a time- and dose-dependent manner. The inhibition of cell growth found in I3C-treated cells may be due to induction of G1 cell cycle arrest as a result of up-regulated p21 expression levels. In agreement with the effect on p21, we found that I3C increases p53 protein expression (Fig. 2a). Since p21 expression is directly induced by the wild-type p53 protein [37], increased p21 expression appears to be dependent of p53 regulation in I3C-treated NALM-6 cells. The growth inhibitory effect of I3C could also be directly related to its ability to down-regulate c-Myc, which is one of the critical molecules required for cell growth and proliferation [38]. We showed that the expression of c-Myc was down-regulated by I3C in NALM-6 cells. Grinkevich et al. have shown in a recent study that p53 ablates c-Myc expression by several mechanisms [39]. Therefore, the up-regulation of p53 induced by I3C may be important in the subsequent down-regulation of c-Myc. It is well established that p53 plays a critical role in protecting against cancer through modulation of various cellular processes including apoptosis, cell cycle arrest, and DNA repair [40]. Mutational inactivation of p53 tumor suppressor gene confers resistance to the chemoradiation therapy that kills cancer cells through apoptotic pathways [41]. Interestingly, TP53 mutations are detected in less than 5 % of pediatric ALL tumors at diagnosis [42, 43]. Given the fact that most cases of BCP-ALL harbor wild-type p53, activation of the p53 pathway by natural dietary agents such as I3C in human ALL cells could be a promising strategy to improve chemotherapy. hTERT is the key component of the human telomerase complex that controls telomerase activity [44]. hTERT expression is repressed in most normal human somatic cells, but high levels of its expression and activity are found in the majority of human tumors [45]. Recent studies have shown that hTERT expression is down-regulated upon activation of wild-type p53 [46]. Notably, it appears that p53-mediated down-regulation of hTERT is important for efficient p53-dependent apoptosis [47]. Moreover, previous studies have demonstrated that the hTERT gene is a direct transcriptional target of c-Myc [48, 49]. Thus, the most straightforward interpretation of our results is that I3C-induced p53 up-regulation and c-Myc down-regulation may contribute in suppression of hTERT expression in NALM-6 cells.

It has been reported that NF-κB is constitutively active in over 90 % of childhood ALL and that the active NF-κB mediates cell survival [16]. In our study, we found that I3C down-

regulates basal activity of NF-κB in NALM-6 cells as shown by decrease in the DNA-binding activity of p65. Our result is consistent with a report by Chinni et al., who showed the suppression of constitutive NF-κB by I3C in PC3 cells [50]. We demonstrated that I3C also inhibited NF-κB-regulated gene products involved in antiapoptosis (IAP1, XIAP, Bcl-2, Bcl-xL) (Fig. 6). Intriguingly, NF-κB is activated in B cell precursor acute lymphoblastic leukemia by treatment with anthracyclines or by ionizing radiation [51]. However, pharmacologic inhibition of NF-κB restores or enhances sensitivity of primary ALL cells to anthracycline-induced apoptosis [52]. Our findings also showed that I3C in combination with doxorubicin was significantly associated with the inhibition of cell proliferation and induction of apoptosis that could be due to the inhibition of nuclear NF-κB p65 expression and NF-κB DNA-binding activity. It has been reported that BCP-ALL cells accumulate high levels of Bcl-2 protein expression which appears to endow lymphoblasts with survival advantage [53]. Furthermore, recent work from the Letai group [54] has indicated Bcl-2 dependency of ALL cells, suggesting the potential ability of Bcl-2 antagonists for improving current ALL therapy. Interestingly, we observed that doxorubicin up-regulated Bcl-2 protein levels in BCP-ALL-derived cell line NALM-6 which was inhibited in the presence of I3C. This finding supports this idea that I3C alone or in combination with anthracyclines may be a useful and novel strategy for the prevention of Bcl-2 expression in BCP-ALL cells.

In summary, we demonstrated that I3C inhibited cell proliferation and induced apoptosis in BCP-ALL cells by simultaneously modulating the p53 and NF-κB signaling pathways.

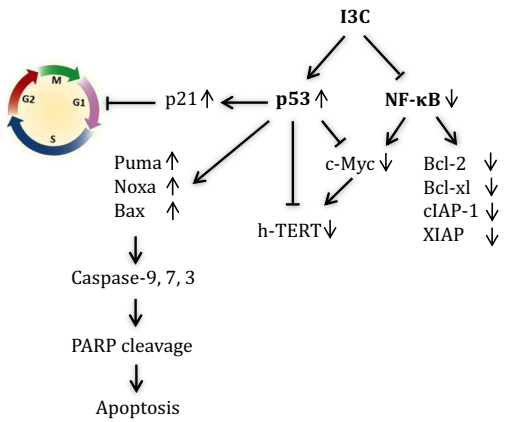

Fig. 6 Schematic representation of the plausible molecular mechanism proposed for the induction of apoptosis by I3C in NALM-6 cells. This molecular mechanism is regulated via the activation of p53 and repression of NF-κB. Subsequently, in response to this activation of p53, the expression of pro-apoptotic p53 target genes Bax, PUMA, and NOXA is enhanced, resulting in the activation of a cascade of caspases and PARP cleavage. p53-mediated p21 up-regulation leads to G1 cell cycle arrest. I3C inhibits protein expression of NF-κB gene products c-Myc, Bcl-2, Bcl-xL, XIAP, and cIAP1 that are involved in cell proliferation and antiapoptosis

Our results showed that combination of lower dose of doxorubicin with a natural nontoxic dietary compound (I3C) enhances the inhibition of cell growth and the induction of apoptosis in NALM-6 cells through inhibition of the NF-κB. Given the pharmacologic safety of I3C, our study suggest that combination of this compound with existing agents will allow a lower dose of chemotherapeutic drugs to be used and thus will decrease nonspecific toxicity of drugs in treatment of BCP-ALL. However, further investigation, including clinical trials, is needed to prove or disprove the usefulness of I3C as either single agent or in combination for the treatment of BCP-ALL.

Acknowledgments This study was supported by the grant 16060 from Iran University of Medical Sciences.

Conflicts of interest None.

References

1. Lo Nigro L. Biology of childhood acute lymphoblastic leukemia. J Pediatr Hematol Oncol. 2013;35:245–52.
2. Stankovic T, Marston E. Molecular mechanisms involved in chemoresistance in paediatric acute lymphoblastic leukaemia. Srp Arh Celok Lek. 2008;136:187–92.
3. Bhojwani D, Pui CH. Relapsed childhood acute lymphoblastic leukaemia. Lancet Oncol. 2013;14:e205–17.
4. Igney FH, Krammer PH. Death and anti-death: tumour resistance to apoptosis. Nat Rev Cancer. 2002;2:277–88.
5. Brown CJ, Lain S, Verma CS, Fersht AR, Lane DP. Awakening guardian angels: drugging the p53 pathway. Nat Rev Cancer. 2009;9:862–73.
6. Wada M, Bartram CR, Nakamura H, Hachiya M, Chen DL, Borenstein J, et al. Analysis of p53 mutations in a large series of lymphoid hematologic malignancies of childhood. Blood. 1993;82:3163–9.
7. Kazemi A, Safa M, Shahbazi A. Rita enhances chemosensivity of pre-b all cells to doxorubicin by inducing p53-dependent apoptosis. Hematology. 2011;16:225–31.
8. Cusack JC, Liu R, Baldwin AS. NF-kappa b and chemoresistance: potentiation of cancer drugs via inhibition of NF-kappa b. Drug Resist Updat. 1999;2:271–3.
9. Tergaonkar V, Pando M, Vafa O, Wahl G, Verma I. P53 stabilization is decreased upon NFkappaB activation: a role for NFkappaB in acquisition of resistance to chemotherapy. Cancer Cell. 2002;1:493–503.
10. Miyamoto S. Rela life and death decisions. Mol Cell. 2004;13:763–4.
11. Perkins ND, Gilmore TD. Good cop, bad cop: the different faces of NF-kappaB. Cell Death Differ. 2006;13:759–72.
12. Wang CY, Cusack Jr JC, Liu R, Baldwin Jr AS. Control of inducible chemoresistance: enhanced anti-tumor therapy through increased apoptosis by inhibition of NF-kappaB. Nat Med. 1999;5:412–7.
13. Panwalkar A, Verstovsek S, Giles F. Nuclear factor-kappaB modulation as a therapeutic approach in hematologic malignancies. Cancer. 2004;100:1578–89.
14. Jost PJ, Ruland J. Aberrant NF-kappaB signaling in lymphoma: mechanisms, consequences, and therapeutic implications. Blood. 2007;109:2700–7.

15. Gasparian AV, Yao YJ, Kowalczyk D, Lyakh LA, Karseladze A, Slaga TJ, et al. The role of IKK in constitutive activation of NF-kappaB transcription factor in prostate carcinoma cells. J Cell Sci. 2002;115:141–51.
16. Kordes U, Krappmann D, Heissmeyer V, Ludwig WD, Scheidereit C. Transcription factor NF-kappaB is constitutively activated in acute lymphoblastic leukemia cells. Leukemia. 2000;14:399–402.
17. Dennis T, Fanous M, Mousa S. Natural products for chemopreventive and adjunctive therapy in oncologic disease. Nutr Cancer. 2009;61:587–97.
18. Aggarwal BB, Ichikawa H. Molecular targets and anticancer potential of indole-3-carbinol and its derivatives. Cell Cycle. 2005;4:1201–15.
19. Rahman KM, Li Y, Sarkar FH. Inactivation of Akt and NF-kappaB play important roles during indole-3-carbinol-induced apoptosis in breast cancer cells. Nutr Cancer. 2004;48:84–94.
20. Choi HS, Cho MC, Lee HG, Yoon DY. Indole-3-carbinol induces apoptosis through p53 and activation of caspase-8 pathway in lung cancer a549 cells. Food Chem Toxicol. 2010;48:883–90.
21. Weng JR, Tsai CH, Kulp SK, Wang D, Lin CH, Yang HC, et al. A potent indole-3-carbinol derived antitumor agent with pleiotropic effects on multiple signaling pathways in prostate cancer cells. Cancer Res. 2007;67:7815–24.
22. Xu D, Wang Q, Gruber A, Bjorkholm M, Chen Z, Zaid A, et al. Downregulation of telomerase reverse transcriptase mRNA expression by wild type p53 in human tumor cells. Oncogene. 2000;19:5123–33.
23. Tapia MA, Gonzalez-Navarrete I, Dalmases A, Bosch M, Rodriguez-Fanjul V, Rolfe M, et al. Inhibition of the canonical IKK/NF kappa B pathway sensitizes human cancer cells to doxorubicin. Cell Cycle. 2007;6:2284–92.
24. Ghosh S, Karin M. Missing pieces in the NF-kappaB puzzle. Cell. 2002;109(Suppl):S81–96.
25. Wang Z, Wang N, Han S, Wang D, Mo S, Yu L, et al. Dietary compound isoliquiritigenin inhibits breast cancer neoangiogenesis via VEGF/VEGFR-2 signaling pathway. PLoS One. 2013;8:e68566.
26. Saldanha SN, Tollefsbol TO. The role of nutraceuticals in chemoprevention and chemotherapy and their clinical outcomes. J Oncol. 2012;2012:192464.
27. Heiduschka G, Lill C, Seemann R, Brunner M, Schmid R, Houben R, et al. The effect of resveratrol in combination with irradiation and chemotherapy: study using merkel cell carcinoma cell lines. Strahlenther Onkol. 2014;190:75–80.
28. Paik WH, Kim HR, Park JK, Song BJ, Lee SH, Hwang JH. Chemosensitivity induced by down-regulation of microrna-21 in gemcitabine-resistant pancreatic cancer cells by indole-3-carbinol. Anticancer Res. 2013;33:1473–81.
29. Licznerska BE, Szaefer H, Murias M, Bartoszek A, Baer-Dubowska W: Erratum to: Modulation of cyp19 expression by cabbage juices and their active components: indole-3-carbinol and 3,3′-diindolylmethene in human breast epithelial cell lines. Eur J Nutr 2014.
30. Chen Z, Tao ZZ, Chen SM, Chen C, Li F, Xiao BK. Indole-3-carbinol inhibits nasopharyngeal carcinoma growth through cell cycle arrest in vivo and in vitro. PLoS One. 2013;8:e82288.
31. Reed GA, Peterson KS, Smith HJ, Gray JC, Sullivan DK, Mayo MS, et al. A phase i study of indole-3-carbinol in women: tolerability and effects. Cancer Epidemiol Biomarkers Prev. 2005;14:1953–60.
32. Bradlow HL, Michnovicz JJ, Halper M, Miller DG, Wong GY, Osborne MP. Long-term responses of women to indole-3-carbinol or a high fiber diet. Cancer Epidemiol Biomarkers Prev. 1994;3:591–5.
33. Takada Y, Andreeff M, Aggarwal BB. Indole-3-carbinol suppresses NF-kappaB and ikappabalpha kinase activation, causing inhibition of expression of NF-kappaB-regulated antiapoptotic and metastatic gene products and enhancement of apoptosis in myeloid and leukemia cells. Blood. 2005;106:641–9.
34. Lyn-Cook BD, Mohammed SI, Davis C, Word B, Haefele A, Wang H, et al. Gender differences in gemcitabine (gemzar) efficacy in cancer cells: effect of indole-3-carbinol. Anticancer Res. 2010;30:4907–13.
35. Cover CM, Hsieh SJ, Cram EJ, Hong C, Riby JE, Bjeldanes LF, et al. Indole-3-carbinol and tamoxifen cooperate to arrest the cell cycle of MCF-7 human breast cancer cells. Cancer Res. 1999;59:1244–51.
36. Nakamura Y, Yogosawa S, Izutani Y, Watanabe H, Otsuji E, Sakai T. A combination of indol-3-carbinol and genistein synergistically induces apoptosis in human colon cancer HT-29 cells by inhibiting Akt phosphorylation and progression of autophagy. Mol Cancer. 2009;8:100.
37. Macleod KF, Sherry N, Hannon G, Beach D, Tokino T, Kinzler K, et al. P53-dependent and independent expression of p21 during cell growth, differentiation, and DNA damage. Genes Dev. 1995;9:935–44.
38. Bernard S, Eilers M. Control of cell proliferation and growth by Myc proteins. Results Probl Cell Differ. 2006;42:329–42.
39. Grinkevich VV, Nikulenkov F, Shi Y, Enge M, Bao W, Maljukova A, et al. Ablation of key oncogenic pathways by rita-reactivated p53 is required for efficient apoptosis. Cancer Cell. 2009;15:441–53.
40. Vogelstein B, Lane D, Levine AJ. Surfing the p53 network. Nature. 2000;408:307–10.
41. Vousden KH, Lu X. Live or let die: the cell's response to p53. Nat Rev Cancer. 2002;2:594–604.
42. Gump J, McGavran L, Wei Q, Hunger SP. Analysis of tp53 mutations in relapsed childhood acute lymphoblastic leukemia. J Pediatr Hematol Oncol. 2001;23:416–9.
43. Fenaux P, Jonveaux P, Quiquandon I, Preudhomme C, Lai JL, Vanrumbeke M, et al. Mutations of the p53 gene in B-cell lymphoblastic acute leukemia: a report on 60 cases. Leukemia. 1992;6:42–6.
44. Bodnar AG, Ouellette M, Frolkis M, Holt SE, Chiu CP, Morin GB, et al. Extension of life-span by introduction of telomerase into normal human cells. Science. 1998;279:349–52.
45. Kim NW, Piatyszek MA, Prowse KR, Harley CB, West MD, Ho PL, et al. Specific association of human telomerase activity with immortal cells and cancer. Science. 1994;266:2011–5.
46. Kusumoto M, Ogawa T, Mizumoto K, Ueno H, Niiyama H, Sato N, et al. Adenovirus-mediated p53 gene transduction inhibits telomerase activity independent of its effects on cell cycle arrest and apoptosis in human pancreatic cancer cells. Clin Cancer Res. 1999;5:2140–7.
47. Rahman R, Latonen L, Wiman KG. hTERT antagonizes p53-induced apoptosis independently of telomerase activity. Oncogene. 2005;24:1320–7.
48. Wu KJ, Grandori C, Amacker M, Simon-Vermot N, Polack A, Lingner J, et al. Direct activation of tert transcription by c-MYC. Nat Genet. 1999;21:220–4.
49. Greenberg RA, O'Hagan RC, Deng H, Xiao Q, Hann SR, Adams RR, et al. Telomerase reverse transcriptase gene is a direct target of c-MYC but is not functionally equivalent in cellular transformation. Oncogene. 1999;18:1219–26.
50. Chinni SR, Li Y, Upadhyay S, Koppolu PK, Sarkar FH. Indole-3-carbinol (I3C) induced cell growth inhibition, G1 cell cycle arrest and apoptosis in prostate cancer cells. Oncogene. 2001;20:2927–36.
51. Weston VJ, Austen B, Wei W, Marston E, Alvi A, Lawson S, et al. Apoptotic resistance to ionizing radiation in pediatric B-precursor acute lymphoblastic leukemia frequently involves increased NF-kappaB survival pathway signaling. Blood. 2004;104:1465–73.
52. Avellino R, Romano S, Parasole R, Bisogni R, Lamberti A, Poggi V, et al. Rapamycin stimulates apoptosis of childhood acute lymphoblastic leukemia cells. Blood. 2005;106:1400–6.

53. Coustan-Smith E, Kitanaka A, Pui CH, McNinch L, Evans WE, Raimondi SC, et al. Clinical relevance of BCL-2 overexpression in childhood acute lymphoblastic leukemia. Blood. 1996;87:1140–6.

54. Del Gaizo MV, Schlis KD, Sallan SE, Armstrong SA, Letai A. BCL-2 dependence and ABT-737 sensitivity in acute lymphoblastic leukemia. Blood. 2008;111:2300–9.